RATE DEPENDENCY DURING PROCESSING OF GLASS/THERMOPLASTIC COMPOSITES

C.E. Wilks[1], C.D. Rudd[1], A.C. Long[1], C.F. Johnson[2]

[1] *School of Mechanical, Materials, Manufacturing Engineering & Management, Division of Mechanical Engineering, University of Nottingham*
University Park, Nottingham NG7 2RD, UK
[2] *Ford Motor Company, Scientific Research Laboratories, Dearborn, MI., 48121, USA*

SUMMARY:

A thermoplastic composite consisting of a polypropylene matrix and aligned glass reinforcing fibres was investigated for the effect of increased forming rates on the deformation mechanism, intraply shearing and the effect of consolidation rate on the void content. It was found that shear thinning of the matrix permitted increased shear rates with minimum force penalties but the void content at the end of consolidation increased with consolidation rate.

KEYWORDS: thermoplastic composite, commingled glass/polypropylene, thermoforming.

INTRODUCTION

The lack of a cost effective, high volume manufacturing process for structural components has been one of the major limiting factors in the proliferation of weight saving composite components for high volume vehicles. Current research is directed towards low cost materials and short cycle time composite processing using highly drapable textile reinforcements combined with thermoplastic matrices such as polypropylene to produce structural components. The primary mechanisms occurring during the stamping of aligned thermoplastic composites (TPCs), during a typical thermoforming cycle are as follows:

1. Intraply shearing to facilitate fabric deformation.
2. Interply shearing for shape accommodation if two or more plies are used.
3. Viscous-friction between the plies and tool surfaces.
4. Pressure application for consolidation of the material to the new shape.
5. Removal of heat to permit solidification of the thermoplastic matrix.

The research presented in this paper describes the effect of rapid forming on the intraply shearing of aligned TPCs and the effect of increasing consolidation rates on the void content in aligned TPCs. In addition, a model that predicts the shear forces as a function of rate was developed and an outline of the requirements for modelling consolidation and void elimination in TPCs is presented. The TPC used for the investigations was a 2 x 2 twill weave of Vetrotex Twintex® commingled E-glass and polypropylene yarn, giving a final glass

volume fraction of 0.35. The mass fractions were 60% glass and 40% polypropylene. It was used in the pre-consolidated form for the intraply shearing investigations and as unconsolidated fabric for the consolidation research.

INTRAPLY SHEARING

The sheet forming process for TPCs involves a number of mechanisms such as intraply and interply shear, resin percolation and transverse squeeze flow. Accommodation of double curvature by a single ply of composite reinforcement is primarily by intraply shear. Although the mechanisms of resin percolation and transverse squeeze flow belong predominantly to consolidation, they also occur as the tow cross-sectional shape changes during the compaction phase of intraply shear. A model has been developed by combining the geometry of the fabric unit cell with lubrication by the molten matrix. This approach shows that the rheology of the composite in intraply shear is dependent upon the rheology of the matrix film at the interface between reinforcing tows.

Experimental Method

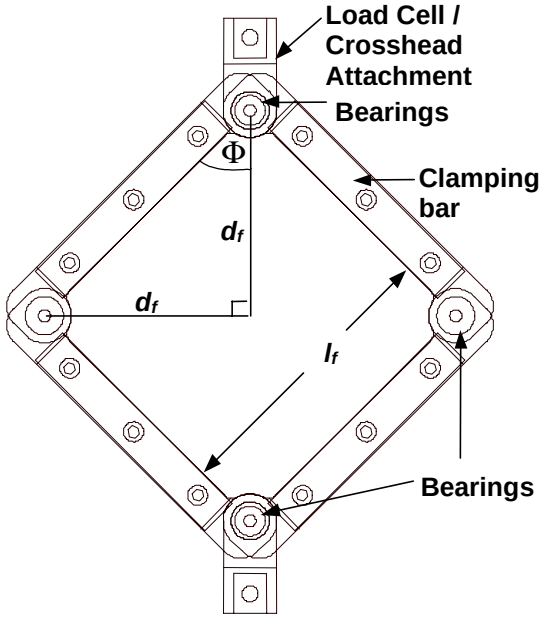

Figure 1 Schematic of the shear rig.

A method of isolating the in-plane deformation mechanism of a composite, intraply shear, is the rhombus-shear or picture-frame shear test (Figure 1). This technique provides homogeneous shearing deformation with no tendency for fibre straightening. The rig was attached to a Hounsfield Universal Mechanical Tester, model H25K-S, having a 1kN load cell. Testing was performed inside an environmental chamber at temperatures of 190°C, 205°C and 220°C and loading rates of 50 to 1000mm/min.

Non-orthogonal tows, due to the pre-consolidating calendering process, develop axial strain during a shear test resulting in higher shear forces [1]. This factor caused substantial variation in results mitigating numerous tests to be performed for each set of conditions. A mean result was calculated from a minimum of six successful tests with error bars indicating the 90% confidence interval using the student *t* test.

Analysis of Shear Test

The shear angle can be expressed as:

$$\gamma = 90 - 2\Phi \tag{1}$$

where Φ is the geometry dependent frame angle shown in Figure 1. The shear force (F_s) is defined as:

$$F_s = \frac{F_{XHD}}{2\cos\Phi} \tag{2}$$

and F_{XHD} is the load recorded by the load cell. The shear rate, $\dot{\gamma}$, is determined by:

$$\dot{\gamma} = \frac{\dot{D}}{l_f \sin\left(\frac{\pi}{4} - \frac{\gamma}{2}\right)} \tag{3}$$

where $\dot{D}$ is the crosshead displacement rate and l_f the distance between adjacent rotary joints.

Results and Discussion

The force required to shear the composite at a given temperature increased with displacement rate and for a givene displacement rate, decreased with temperature as shown in Figure 2.

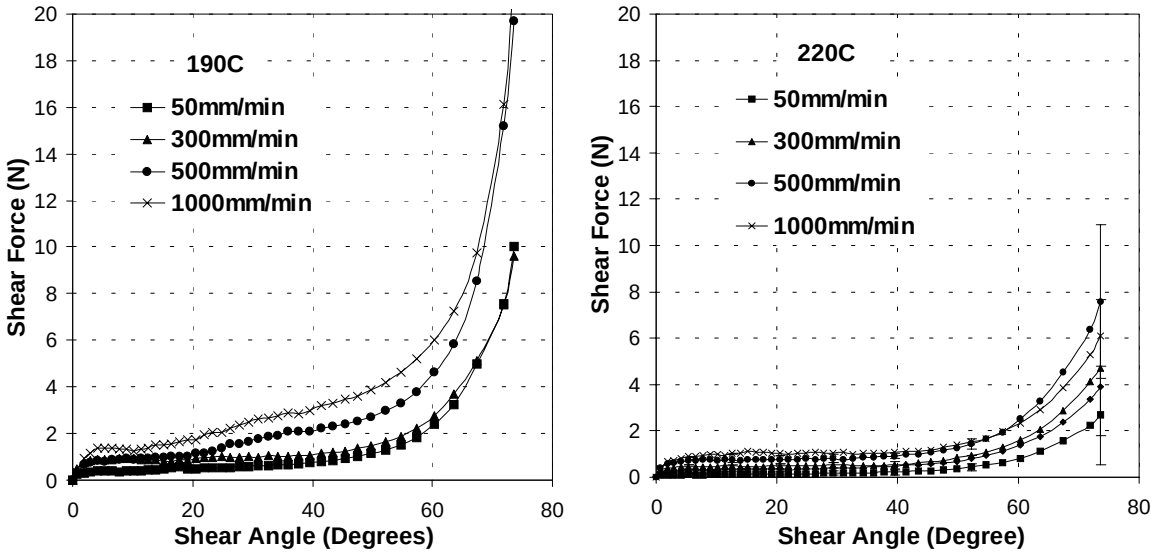

Figure 2 Shear force v shear angle for pre-consolidated commingled fabric at 190°C and 220°C.

Figure 3 shows the increasing shear force with load rate at four shear angles for the specimens tested at 205°C. The shape of these curves indicate that the matrix behaves as a Newtonian fluid at load rates up to approximately 200mm/min, beyond which, non-Newtonian shear thinning occurs. The points for 1000mm/min in Figure 5 indicate that a rapid increase in the shear force had commenced. The magnitude of the difference between these points and the 800mm/min points may be exaggerated due to the contribution of non-orthogonal fibres in the samples tested. However, the increase may be due to limits in the shear thinning of the polypropylene matrix at the tow/tow interfaces. Further shear rate increases would result in further shear force increases.

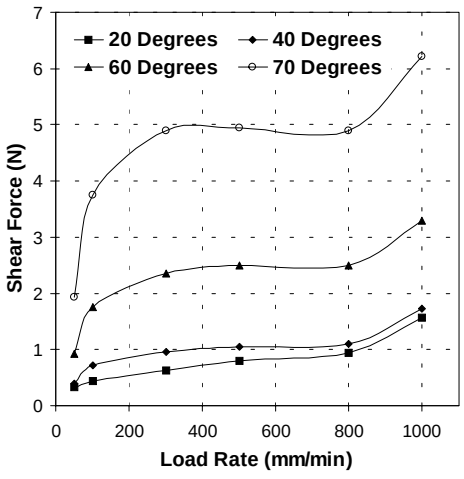

Figure 3 Shear force versus load rate for four shear angles at 205°C.

Modelling Intraply Shearing

McGuinness and O'Bradaigh [2] modelled intraply shear using the constitutive equations for an Ideal Fibre Reinforced Fluid developed by Spencer [3]. The model was developed to predict the viscosity of the composite. However, the viscosities predicted by this model were

often substantially higher than the neat matrix viscosity.The model presented here determines the shear forces as a result of the matrix viscosity at the interface between tows. The deformation during intraply shear is considered to consist of three separate mechanisms:

1. At the crossover interface of warp and weft tows, a film of matrix separates the two tows, providing resistance to rotation.
2. Two adjacent tows are initially in intimate contact along their edges. Resistance to movement in the axial direction of one tow relative to the other tow is by a matrix film at the tow/tow interface
3. During shearing the tow changes shape which requires a mass transfer of matrix and fibres.

The third mechanism involves very short flow distances and the resistance to tow shape change is assumed to be negligible. Therefore, of these three contributing mechanisms it is considered that the first two are quantitatively more important.

Contribution of Tow Rotation at the Crossover

It is assumed that the sum of the crossover contact areas is equal to the area of the sample and that the sample is a balanced weave. A circle of equivalent area and a diameter termed the effective diameter, D_{eff}, may describe the crossover area. The relative velocity of the tows is calculated from geometric considerations. Consider an arc on the perimeter of the equivalent circle. For rotation at a crossover due to a shear angle γ, the arc length *s* is given by:

$$s = \frac{D_{eff}}{2}\gamma \tag{4}$$

Therefore, the velocity of the crossover as it rotates through arc *s* is given by:

$$\frac{ds}{dt} = \frac{ds}{d\theta}\cdot\frac{d\gamma}{dt} \text{ where } r = \frac{ds}{d\theta} \tag{5}$$

The shear angle and shear rate of the picture frame rig are given by Equations 1 and 3. Integrating over the total crossover area for gives the average velocity by:

$$\dot{s}_{AV} = \frac{\dot{\gamma}}{A}\int_0^A r\, dA \tag{6}$$

$$\dot{s}_{AV} = \frac{D_{eff}}{3}\dot{\gamma} \tag{7}$$

The product of the velocity gradient, $\frac{dv}{dx}$, through the film of matrix, of thickness *h* and the viscosity, η, at the interface determines the shear stress at the crossover.

$$\tau = \eta\frac{dv}{dx} = \eta\frac{D_{eff}}{6h}\dot{\gamma} \tag{8}$$

The torque at the crossover can be calculated by using Equation 8. The total torque on the frame results from contributions of the crossover shear forces, F_{sx}, and the shear forces developed by the realitve motion of adjacent tows, F_a. An expression whereby the torque on the frame due to F_{sx} is equivalent to the sum of the torque at each crossover is then rearranged to find the value for F_{sx} as shown by Equation 9 where *l* is the crossover dimension and l_f is the sample dimension as shown in Figure 1.

$$F_{sx} = \frac{\eta\, l^2\,\dot{\gamma}\, l_f \cos\gamma}{6h\pi} \tag{9}$$

Contribution of the Relative Motion of Adjacent Tows to the Shear Force

The commingled fabric is a 2x2 twill weave. Unlike a plain weave, the edges of adjacent warp tows in the twill weave are in intimate contact over a distance equal to the tow width for every two weft tows that are crossed. The same contact length occurs in the weft direction.

Therefore, the initial contact length between adjacent tows in either direction, is one tow width, *l*, in every two tow widths. As intraply shearing proceeds, the initially flat tow becomes oval due to the compacting forces as the total sample surface area decreases. Therefore, the short transverse thickness, $t_{initial}$, increases and the width decreases. In addition to the thickness increase, the contact length also increases as the distance between the two perpendicular tows bordering the ends of the original contact length effectively move apart as their width decreases. Hence the total contact area, A_c, as a function of shear angle is given by:

$$A_c = \left(\frac{l_f}{2l}\right)^2 (2l - l\cos\gamma)\frac{t_{initial}}{\cos\gamma} \tag{10}$$

The contribution by the adjacent tow contact to the total shear force, F_{sa}, is found by addition of the individual shear forces between adjacent tows.

$$F_{sa}\frac{l_f}{2}\cos\gamma = \sum_{n=1}^{l_f/2l} F_a.nl\cos\gamma \tag{11}$$

The shear force between adjacent tows, F_a, is the product of the velocity gradient and the viscosity in the matrix film at the interface. Rearrangement of Equation 11 following substitution for F_a and the summation for all *n* gives:

$$F_{sa} = \eta\frac{\dot{\gamma}\, l_f\, t_{initial}\, l}{4h}(2-\cos\gamma)\frac{1}{2}\left(\frac{l_f}{2l}\right)\left[\left(\frac{l_f}{2l}\right)+1\right] \tag{12}$$

Total Shear Force

The addition of Equations 9 and 12 predicted shear forces that were higher than the experimental shear forces shown in Figure 2. The model assumes the tows have complete and constant contact at the interfaces. In reality, tows have curved surfaces and are separated by a film of matrix of irregular and dynamic thickness. Factors have been calculated empirically to accommodate the geometric variations occurring during shearing of the composite. The factors approximate the fraction of the ideal interface contact that actually occurs. Values for the geometric factors in Equation 13 were found to be 0.5 for the crossover term, GF_x and 0.025 for the adjacent tows term, GF_a.

$$F_s = GF_x.\eta\frac{l^2\dot{\gamma}\, l_f\cos\gamma}{6h\pi} + GF_a.\eta\frac{\dot{\gamma}\, l_f^2\, t_{initial}}{16h}(2-\cos\gamma)\left[\left(\frac{l_f}{2l}\right)+1\right] \tag{13}$$

Figure 4 shows the predicted shear force curves for the conditions used for the experimental results shown in Figures 2. Compaction during intraply shearing causes resin percolation that may decrease the matrix film thickness. This was observed as beading of the matrix on the surface of the sample. Increasing shear rate, temperature and normal pressure all decrease the film thickness. Therefore, a relationship between film thickness and shear angle was considered appropriate as both shear rate and normal pressure increase with shear angle for the picture frame shear test. Due to a lack of experimental data for the initial thickness and the reduction in matrix thickness, an empirical relationship was developed using an estimate for the initial thickness:

$$h = h_{initial}(\cos\gamma)^m \tag{14}$$

The value for *m* was determined empirically to be 0.35 for all temperatures. This value was based on the assumption that the initial matrix thickness was unaffected by temperature, which may not be the case in practice. Equation 13 predicts that the shear force increases with shear rate and decreases as temperature increases. For each load rate tested over three temperatures, the predicted shear force and the experimental shear force showed very good correlation.

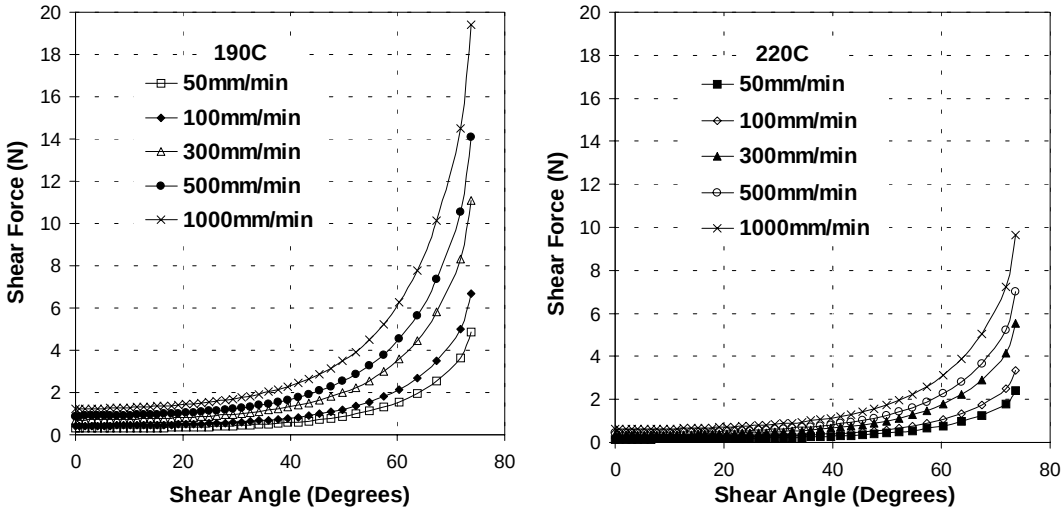

Figure 4 Predicted shear force versus shear angle at 190°C and 220°C.

CONSOLIDATION AND VOID REDUCTION

The final phase in the manufacture of TPC components is consolidation of the composite and void reduction. During consolidation of a commingled thermoplastic/glass fabric the matrix is required to flow very short distances for impregnation of the reinforcement. Consolidation appears to be the rate-determining step of the overall process, hence, prediction of the consolidation time for given temperature, pressure and rate parameters has been the focus of models presented by various researchers [4-9]. Although, modelling a process as complicated as the consolidation of TPCs requires considerable simplification of the mechanisms involved, it remains essential to maintain the physical phenomena as the basis for any model. One approach has been to adapt models developed for liquid moulding processes such as resin transfer moulding. In this section it will be shown that this approach is limited to a small, although essential part of the overall consolidation phase.

The objectives were to determine:

1. The various mechanisms that constitute the consolidation phase and present these findings as the basis of an integrated modelling approach.
2. The effect of consolidation rate on void content.
3. The processing window required for rapid consolidation of a glass fibre/polypropylene commingled fabric to a specified maximum void content.

The approach taken to achieve these objectives includes an analysis of laminate thickness as a function of consolidation rate, the effect of temperature on the required pressure to achieve a given laminate thickness and the void content as a function of holding pressure during cooling. To determine the various mechanisms or phases during consolidation and void elimination, microstructural samples at various stages were analysed.

Experimental Method

The consolidation rig consisted of a heated circular upper platen of 50mm diameter and a heated 115mm^2 lower platen (Fig. 5). Fabric was clamped to the base platen by a 115mm^2 plate containing a hole of diameter 50.16mm, providing a 0.08mm shear edge with the upper tool. The clamping plate prevented matrix outflow from beneath the platen. Testing was performed in a Hounsfield Universal Mechanical Tester Model H25K-S using 1kN and 25kN load cells at loading rates of 1 to 50mm/min. Samples consisted of two plies of fabric with a

theoretical fully consolidated thickness of 1mm per ply. The temperature of the platens was maintained at 200°C. Samples were stabilised at the test temperature for 4-4.5 minutes prior to consolidation. A linear variable differential transducer (LVDT) measured the platen displacement. The final results are the average of a minimum of six samples that exhibited good repeatability. A Student's t-test at the 90% confidence level was applied to each data set for calculation of the error margin. Void contents were measured by image analysis. Two test routines were employed:

1. Constant displacement rate to the load cell maximum of either 1kN or 25kN.
2. Constant displacement rate to a predetermined load, which was then maintained during cooling.

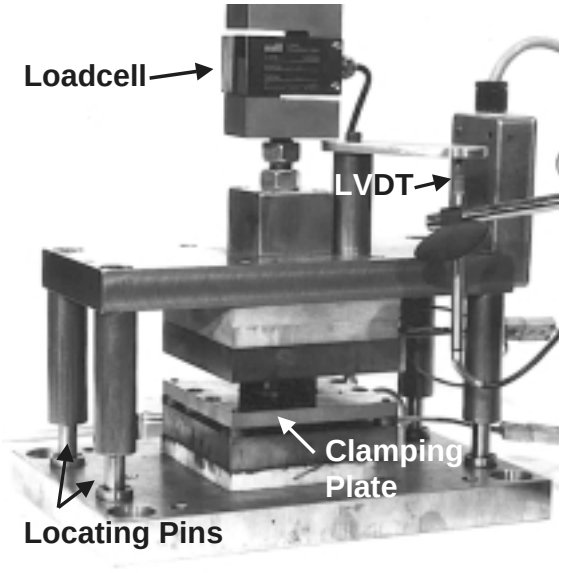

Figure 5. Compaction tool showing the positions of the four locating pins and the LVDT.

Results and Discussion

Figure 6 shows the results for constant consolidation rates of 0.2 to 50mm/min at 200°C. The curves were produced using a 1kN load cell for rates up to 25mm/min and a 25kN load cell for rates above 25mm/min. The degree of consolidation is given as a normalised thickness, which is the inverse of the ratio of laminate thickness to the predicted thickness at zero voidage. At rates of 35mm/min and above, there was consolidation to a normalised thickness of approximately 0.82 before a rapid increase in pressure to the load cell maximum of 12.7 MPa, with minimal associated gain in consolidation. This pseudo-asymptotic effect can also be visualised for the rates below 35mm/min by extrapolation of the curves in Figure 6. This extrapolation suggests that the asymptotic normalised thickness achieved at 15mm/min and below would be greater than for rates above 15mm/min. Hence, before the pressure increased rapidly, a lower void content would result for rates below 15mm/min than for those above this rate. Figure 7 illustrates this more clearly by plotting pressure versus rate for a normalised thickness of 0.8. Initially there is a rapid pressure increase corresponding to the linear Newtonian behaviour of polypropylene at low shear rates, followed by a levelling of the pressure whilst polypropylene undergoes shear thinning before a linear rapid increase in pressure due to viscoelastic effects within the polypropylene matrix.

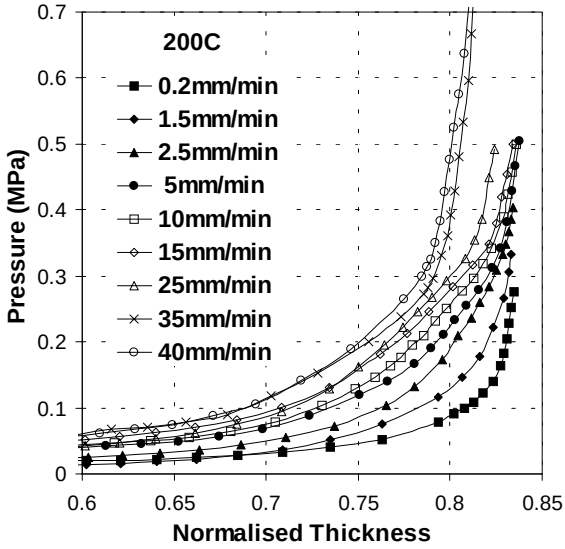

Figure 6 Pressure versus normalised thickness.

The effect of maintaining pressure during cooling of the laminates was investigated by analysis of the void content using image analysis techniques. Laminates were prepared using the constant load test routine. Samples were consolidated at constant rates of 5 and 30mm/min

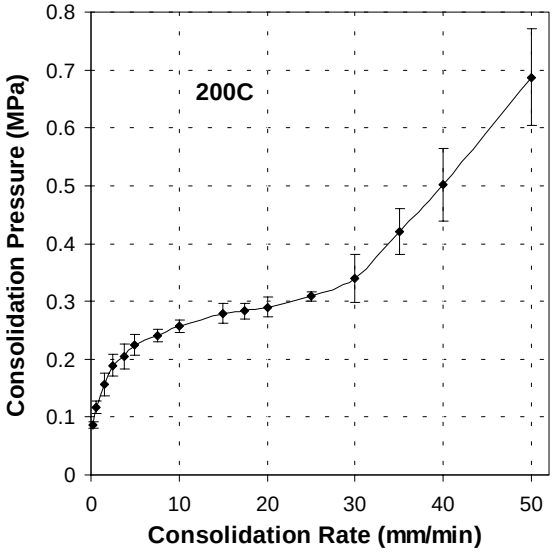

Figure 7 Pressure v consolidation rate at 200°C for a normalised thickness of 0.8.

Analysis of the effect of temperature upon the required pressure for consolidation was undertaken in two steps. The first step was a straightforward approach using the constant displacement rate test routine for temperatures 180°C to 220°C in steps of 10°C. Samples were heated to these temperatures and then consolidated. The second step required heating to 200°C followed immediately by cooling at 7°C/min to the test temperature. Results for values at a normalised thickness of 0.8 are shown in Figure 9. Extrapolation of the curve for specimens consolidated without cooling would result in a very rapid increase in pressure as the melt temperature of 165°C was approached. However, the polypropylene matrix solidifies substantially below the melt temperature as shown by the curve for specimens that were cooled from 200°C prior to consolidation.

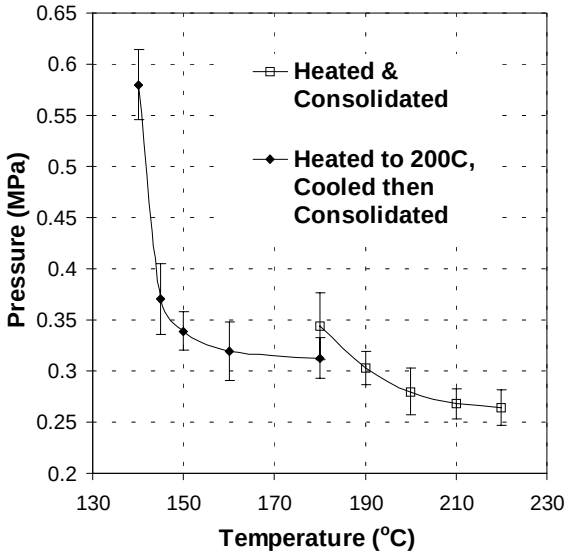

Figure 9 The effect of super cooling on the processing window of polypropylene based TPCs.

to the predetermined pressure, at which point the laminate was cooled at a rate of 7°C/min, whilst the pressure was maintained. The measured void contents are shown in Figure 8. This confirmed the decrease in asymptotic normalised thickness as the consolidation rate increased, as suggested by Figure 6.

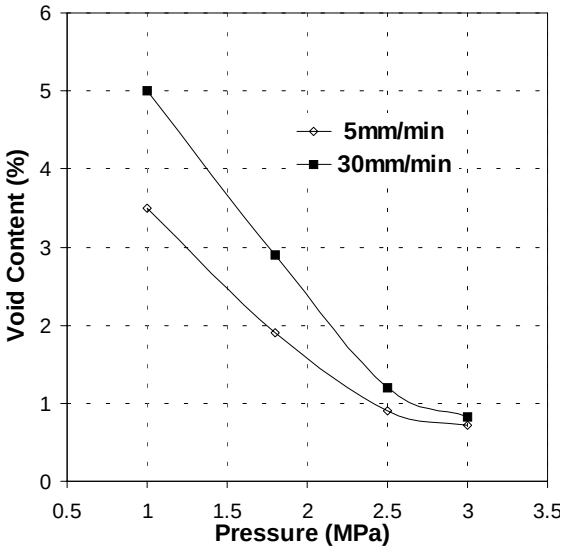

Figure 8 Void content v pressure for laminates consolidated at 5 and 30mm/min followed by cooling under pressure.

The microstructures of two plies were analysed at different stages of consolidation, from heating to 200°C and cooling without applied pressure, through to consolidation to a void content less than 1%. The sequence of compaction and consolidation observed and possible approaches to modelling are as follows:

1. *Initial coalescence of the molten matrix before application of pressure (Figure 10). No consistent pattern of matrix flow from the fibre bundles.* A method to predict the fibre bundle void content at the end of preheating would be

based on initial measurement of the degree of commingling within the commingled yarn after processing into a woven fabric.

2. *Coincident removal of air from between the plies and within the plies as pressure is applied.*

3. *Entrapment of air as escape paths to the surfaces are closed by molten matrix.* Prediction of the quantity of air that is entrapped between the plies as escape path closure occurs during this phase may be empirical. The amount of entrapped air determines the time and/or pressure during the time at pressure phase for void reduction.

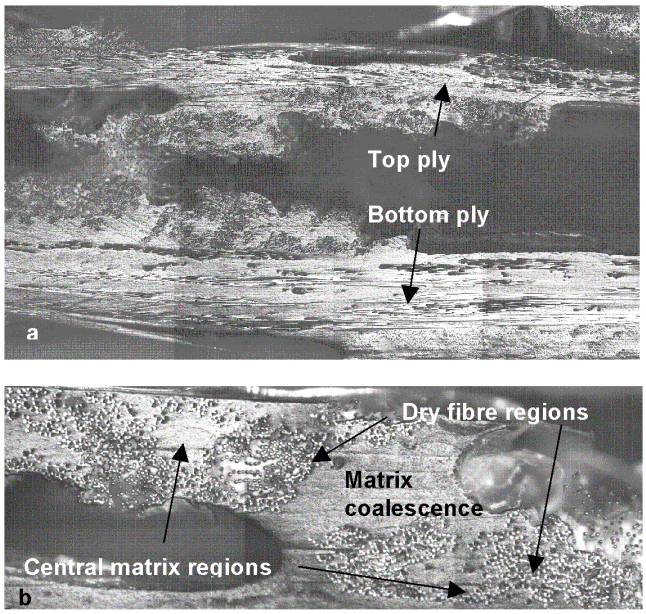

Figure 10 a. Microstructure following heating to 200°C and cooling without applied pressure.
b. A region showing two separate tows containing a central resin rich area and two adjacent matrix depleted regions

4. *Reduction in the volume of the entrapped air as the pressure rises more rapidly. Compaction of the tows as the applied pressure increases.* Compaction of the tows causes matrix outside the tow to flow transversely into dry areas of the tow. It is this phase that has been modelled by a number of researchers using Darcy's law. However it cannot be assumed that there is no flow longitudinally within the tow. The action of the compacting fibres may force the matrix present within the tow to flow longitudinally into voids more readily than matrix flowing into the tow from the region between tows. Hence, longitudinal flow within the fibre bundle may also require modelling as this, depending on the degree of commingling, may constitute the majority of the fibre bundle "wet-out".

5. *Once consolidation pressure nears the asymptotic value, the voids remaining are predominantly within the matrix rich regions (Figure 11).*

6. *Application of pressure during cooling reduced the void content with remaining voids being in matrix rich regions.* Void reduction is a combination of void volume reduction and dissolution of entrapped gases into the matrix as described by Letterier and G'Sell [10]. Prediction of the void content at the end of consolidation at constant rate is required before a relationship between time, pressure and void content can be developed. This may be empirically or by a combination of void reduction by the equation $P_1V_1 = P_2V_2$ and the dissolution

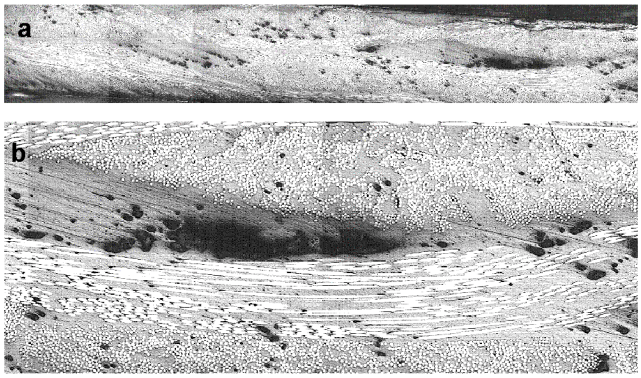

Figure 11 a. Consolidated to a normalised thickness of 0.86.
b. Higher magnification shows the predominance of voids in the matrix rich regions between tows.

kinetics for air into the matrix at the given conditions of temperature and pressure.

Conclusions

Two of the mechanisms involved in the stamping of TPCs have been investigated to determine the effect of incresing the forming and consolidation rates. It was found that the shear thinning of the thermoplastic matrix at the interface between tows prevented high shear forces developing during intraply shearing at increasing rates. This factor may enable the prediction of tow placement and the draping of complex parts during the high rate forming required by TPC stamping. The intraply shearing model demonstrates a physical-based approach for prediction of the forces required.

Consolidation and void elimination for TPCs is a complex process in the absence of a macro matrix flow common to thermoset liquid moulding processes. Modelling of the overall process requires contribution from a number of separate phases. The shear thinning of the matrix controls the effect of consolidation rate, giving an optimum rate for the composite analysed of 5 to 25mm/min. However, it was found that void elimination was determined less by the starting void content, at the end of consolidation, than by the applied pressure. This indicates that the consolidation rate may be superfluous to the pressure level during time at pressure prior to final cooling.

References

1. U.P. Breuer, "Analysis of the Forming of Reinforced Thermoplastics," in *Institut fur Verbundwerkstoffe*. Kaiserslautern: University of Kaiserslautern, 1997, pp. 123.
2. G.B. McGuinness, C.M. O'Bradaigh, "Development of Rheological Models for Forming Flows and Picture-Frame Shear Testing of Fabric Reinforced Thermoplastic Sheets", *Journal of Non-Newtonian Fluid Mechanics*, **73** pp. 1-28 (1997).
3. A.J.M. Spencer, *Deformations of Fibre-Reinforced Materials*. Oxford: Clarendon Press, 1972.
4. T.A. Cain, M.D. Wakeman, R. Brooks, A.C. Long, C.D. Rudd, "Towards an Integrated Processing Model for a Co-mingled Thermoplastic Composite". *Proceedings of ICCM-11*, Gold Coast, Australia, 14-18th July 1997, **5** pp. 366-376.
5. V. Klinkmuller, M.K. Um, M. Steffens, K. Friedrich, B.S. Kim, "A New Model for Impregnation Mechanisms in Different GF/PP Commingled Yarns", *Applied Composite Materials*, **1** pp. 351-371 (1995).
6. L. Ye, K. Friedrich, J. Kastel, "Consolidation of GF/PP Commingled Yarn Composites", *Applied Composite Materials*, **1** pp. 415-429 (1995).
7. B.P.V. West, R.B. Pipes, M. Keefe, S.G. Advani, "The Draping and Consolidation of Commingled Fabrics", *Composites Manufacturing*, **2** [1] pp. 10-22 (1991).
8. V. Klinkmuller, M.K. Um, K. Friedrich, B.S. Kim, "Impregnation and Consolidation for Different GF/PP Commingled Yarn". *Proceedings of ICCM-10*, Whistler, Canada 1995, **3** pp. 397-404.
9. A.H. Miller, N. Dodds, J.M. Hale, A.G. Gibson, "High Speed Pultrusion of Thermoplastic Matrix Composites", *Composites Part A*, **29A** pp. 773-782 (1998).
10. Y. Leterrier, C. G'Sell, "Formation and Elimination of Voids During the Processing of Thermoplastic Matrix Composites", *Polymer Composites*, **15** [2] pp. 101-105 (1994).